



# Quark-Hadron Duality at Large $Q^2$

*Simona Petruta Malace*  
*Hall C Meeting*  
*January 25, 2007*

## Outlook

Theory and Physics context and motivation for experiment E00-116  
Experimental setup  
Data analysis  
Results  
Conclusions



# Quark-Hadron Duality: the Phenomenon

Unsolved problem of the Standard Model of the nuclear and particle physics: understand the structure and interaction of hadrons in terms of QCD degrees of freedom: quarks and gluons.

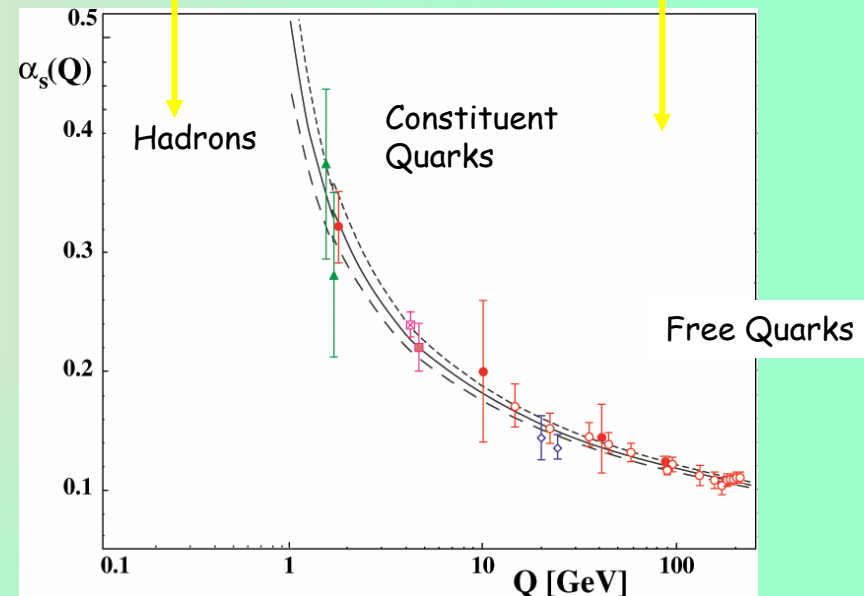
However:

In specific cases (RES) although the description in terms of collective DOF seems more natural, the description in terms of quarks and gluons can also be used with very similar results.

quark-hadron duality

Low energies:  
collective degrees of  
freedom - hadrons  
(RES).

High energies:  
degrees of freedom  
- quarks and gluons  
(DIS).



Connection between confinement and asymptotic freedom.  
Transition between the perturbative and nonperturbative regimes.  
Reason why the parton model works well down to low energy scale.



# Historically: Bloom-Gilman Duality (1970)

The resonance region data:

- \*) oscillate around the scaling curve.
- \*) are on average equivalent to the scaling curve.
- \*) "slide" along the deep inelastic curve with increasing  $Q^2$ .

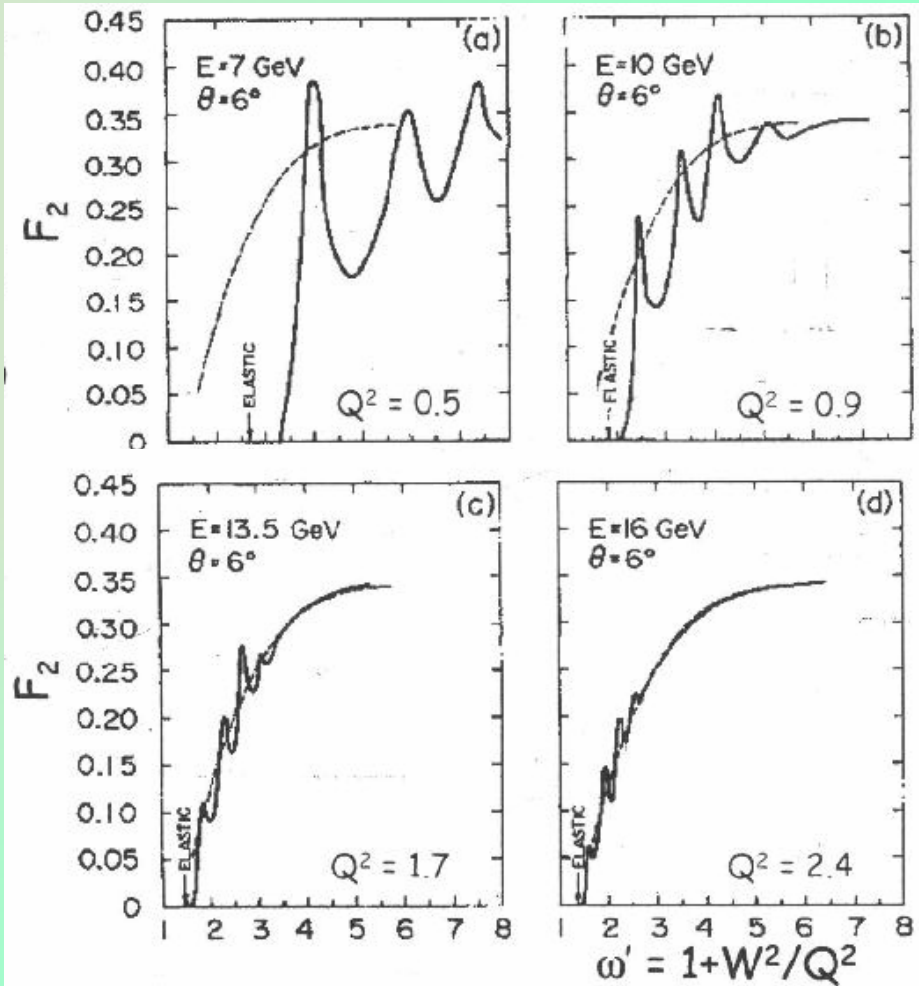
"the resonances are not a separate entity but are an intrinsic part of the scaling behavior"

Finite energy sum rule (pre-QCD era):

$$\underbrace{\frac{2M}{Q^2} \int_0^{v_m} v W_2(v, Q^2) dv}_a = \underbrace{\int_1^{(2Mv_m + m^2)/Q^2} v W_2(\omega') d\omega'}_b$$

a

b



Quantitatively: when comparing a and b, the relative difference ranged from 10% for  $Q^2=1 \text{ GeV}^2$  to <2% for  $Q^2=2 \text{ GeV}^2$ .



# Quark-Hadron Duality in QCD

1976- de Rujula Georgi and Politzer reinterpreted quark-hadron duality in terms of the twist expansion of the moments of the structure function in QCD:

OPE:

$$M_2^{(n)}(Q^2) = \sum_{\tau=2,4,..}^{\infty} \frac{A_{\tau}^{(n)}(\alpha_s(Q^2))}{Q^{\tau-2}}, \quad n = 2,4,6,..$$

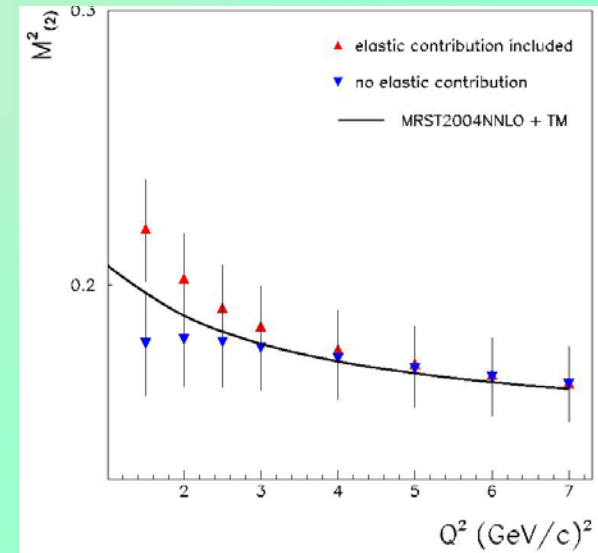
$M_2^{(2)}$  → Bloom-Gilman integral

low  $Q^2$ : large corrections from the subleading higher-twist terms => very strong  $Q^2$  dependence of the moments.

scaling contribution from the leading-twist => shallow  $Q^2$  dependence of the moments.

Duality = higher-twist are either small or cancel (on average, the interactions between the valence quarks are suppressed).

Why?

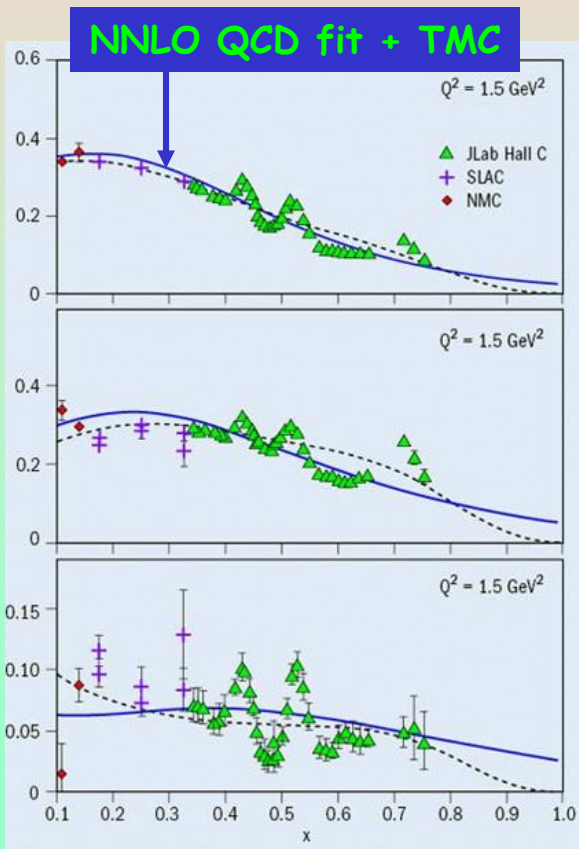
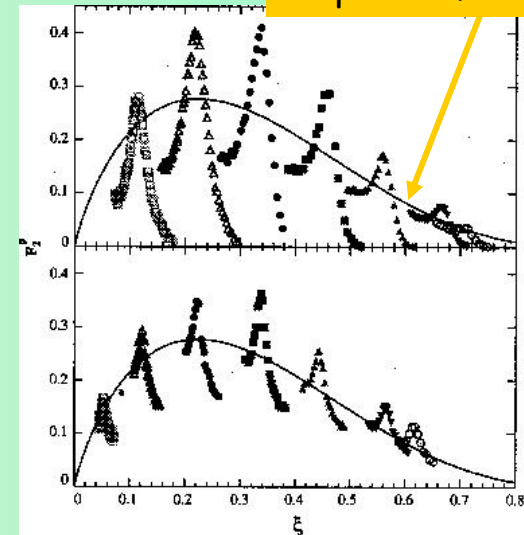




# Quark-Hadron Duality: Experimental Results

Hall C experiment, 1996 (I. Niculescu et al.): revived the interest in quark-hadron duality phenomenon ->

- $\xi$  as scaling variable (accounts for TM effects)
- duality also manifests itself locally, i.e. for each resonance region separately.



E94-110: The resonance region is, on average, well described by **NNLO QCD fits**.

Quantitatively duality works better than 10% at surprisingly low  $Q^2$  ( $0.5 \text{ GeV}^2$ )

“The successful application of duality to extract known quantities suggests that it should also be possible to use it to extract quantities that are otherwise kinematically inaccessible.”

*(CERN Courier, December 2004)*

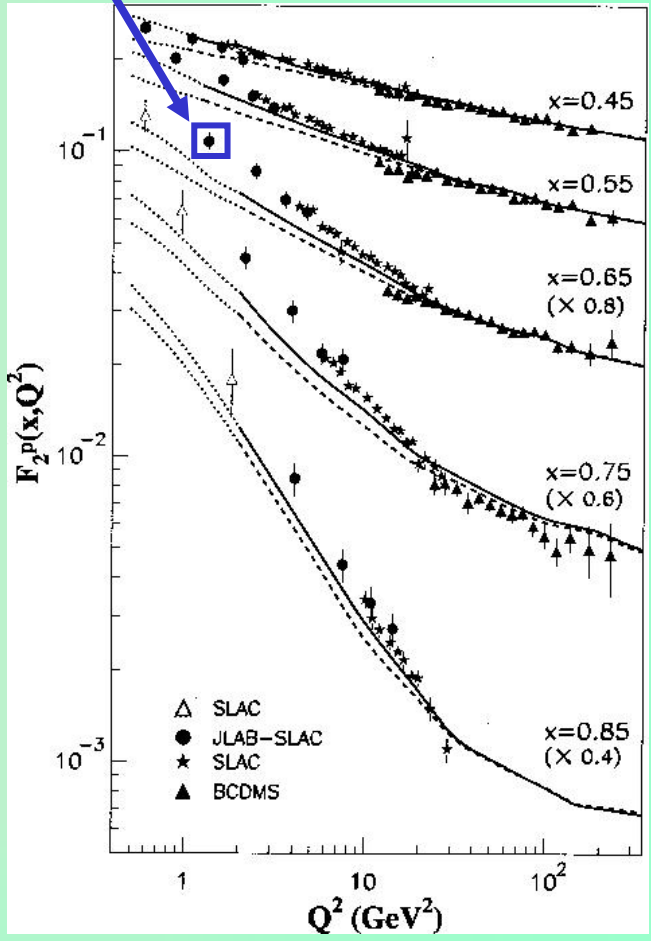
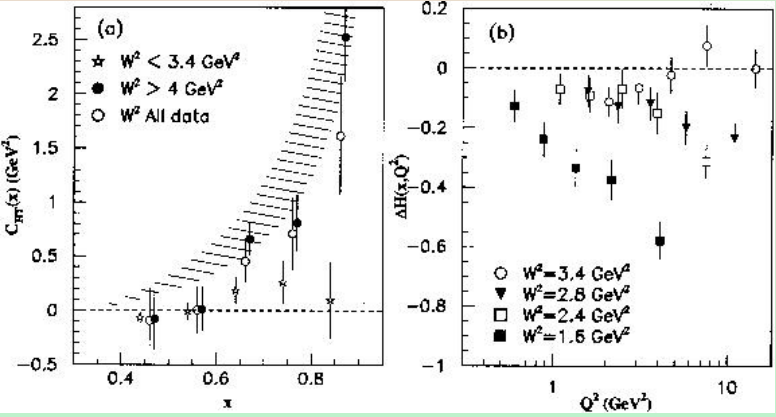


# Cont'd

$1.3 < W^2 < 3.4 \text{ GeV}^2$

S. Liuti, R. Ent, C. E. Keppel, I. Niculescu,  
Phys. Rev. Lett. 89 (2002) 162001

$Q^2$ -evolution of  $F_2$  compared to NLO QCD fit + TM + LxR  $\Rightarrow$  LxR effects improve the agreement data-QCD fit. The remaining discrepancy assumed to be due to dynamical higher-twist effects.



pQCD leading twist + TM + LxR

$$\frac{F_2^{\text{exp}}}{F_2^{\text{pQCD+TM}}} = 1 + \frac{C_{HT}(x)}{Q^2}$$

$$\frac{F_2^{\text{exp}}}{F_2^{\text{pQCD+TM}}} = 1 + \frac{C_{HT}(x)}{Q^2} + \Delta H(x, Q^2)$$

CHT and  $\Delta H(x, Q^2)$  dynamical higher-twists  
CHT in RES region similar but smaller than CHT in DIS

...But this makes sense if duality holds:  $\Delta H(x, Q^2)$  is negative for each resonance region



# E00-116 Physics Motivation

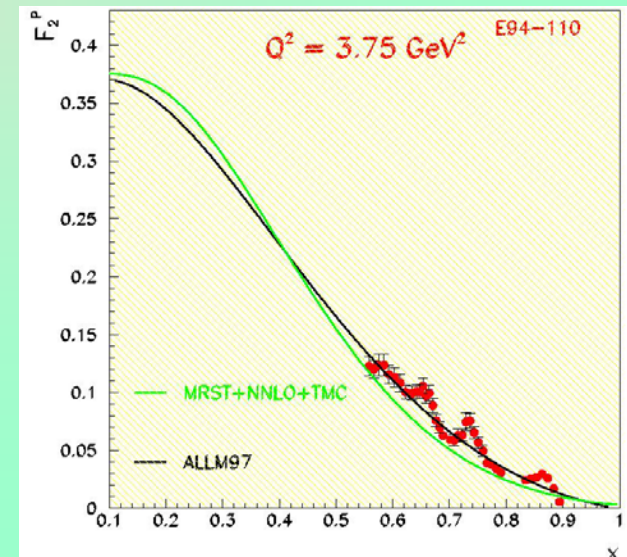
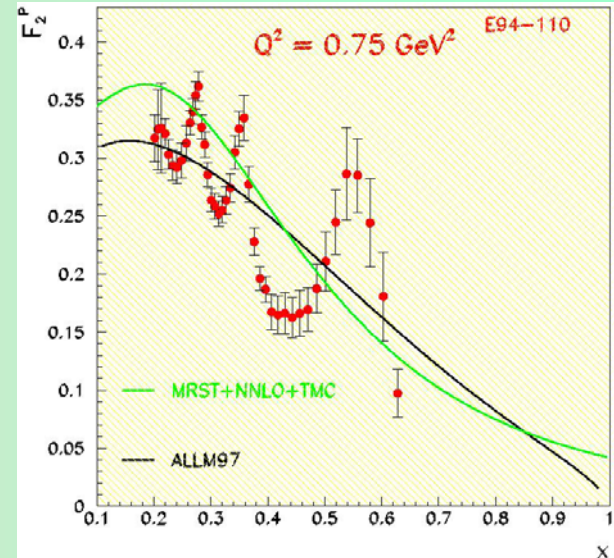
Higher twist extraction from both  $H_2$  and  $D_2$  data.

Constrain higher moments.

With increasing  $Q^2$  the resonances slide towards higher  $x$  on DIS empirical curve (ALLM97) while the Parton distribution function (pdf) curve MRST+NNLO+TMC starts undershooting the data.



Constrain large  $x$  quark distributions evolution





# Experimental Setup

## Beam:

**E00-116:** energy ( $E$ ) = 5.5 GeV, current ( $I$ ) up to  $100\mu A$

## Target:

**LH<sub>2</sub>** target (19 K) = liquid hydrogen in an aluminum can

**LD<sub>2</sub>** target (22 K) = liquid deuterium in an aluminum can

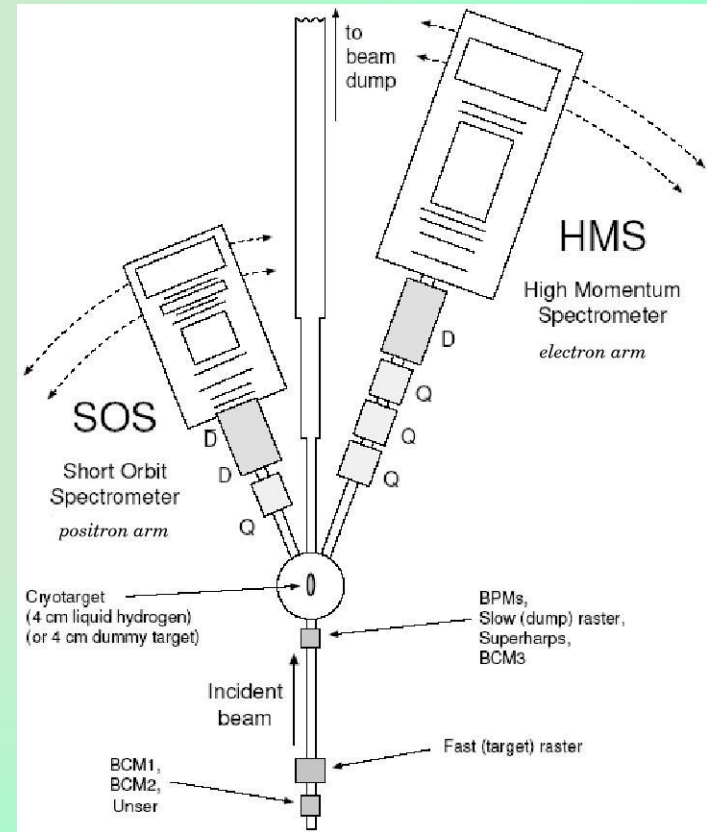
**Al** target (dummy) for background measurements

Effective target length obtained through:

- target survey
- target position relative to the pivot
- beam offset relative to the pivot

## Spectrometer:

**HMS** for inclusive  $e^-$  detection; **SOS** for positron measurements



Accumulated (mainly) **RES** region data with:

$$Q^2 \in (3.88 - 7.21) \text{ GeV}^2$$

$$x \in (0.54 - 0.94)$$



# Methodology of Cross Section Extraction

differential Born cross section

$$\frac{d\sigma}{d\Omega dE'} = (N_{measured} - BG) \frac{1}{N_e N_t} \frac{1}{\Delta\Omega \Delta E'} \frac{1}{A} \frac{1}{\epsilon}$$

$\epsilon$ : Total efficiency for detection

- Electronic and computer life time
- Trigger and Tracking efficiency
- Cerenkov and Calorimeter detector efficiency

$A(E', \theta)$  = acceptance, i.e. the probability that a particle will make it through the spectrometer and *was determined from simulation!*

## Background

- $e^-$  scattered from Al walls of cryogenic target cell.
- $e^-$  from charge-symmetric  $\pi^0, \gamma$  production and decay.
- $e^-$  from radiative events.
- $\pi^-$

## Eliminate by

- Subtracting measured  $e^-$  from Al dummy target.
- Subtracting measured  $e^+$  yields.
- Applying radiative corrections.
- Cerenkov and calorimeter cuts.

Iterations and model dependence of the extracted cross sections. 



# Charge Symmetric Background Calculation

We used **SOS** for H,D ( $e, e^+$ ) measurement.

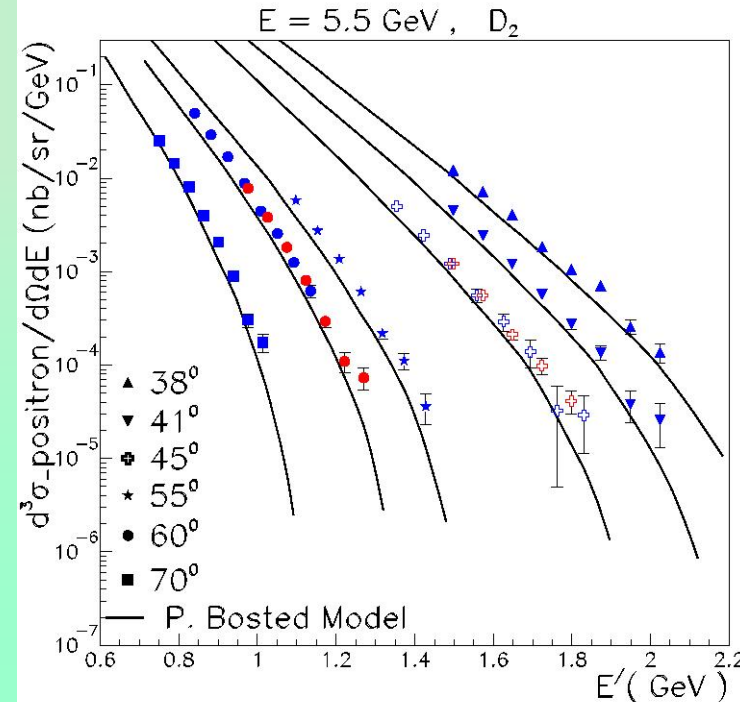
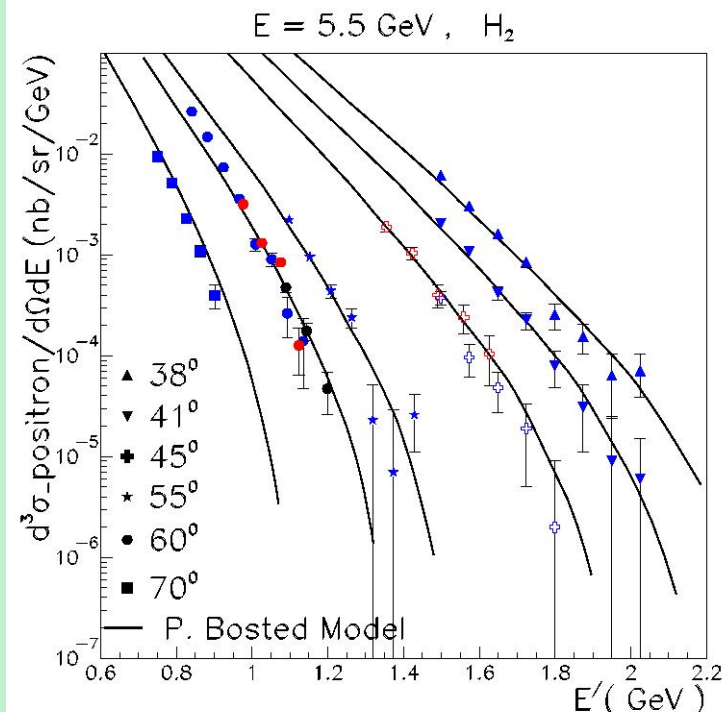
SOS has a larger acceptance than HMS. ( $e, e^+$ ) cross section is varying strongly as a function of  $\theta$  and  $E'$ . Therefore we need to disentangle  $\theta$  and  $E'$  dependence in order to do the subtraction.

To calculate positron cross sections:

- tracking inefficiency
- dead time(e.d.t & c.d.t)
- dummy subtraction
- pion contamination
- acceptance corrections
- bin centering (P. Bosted model-

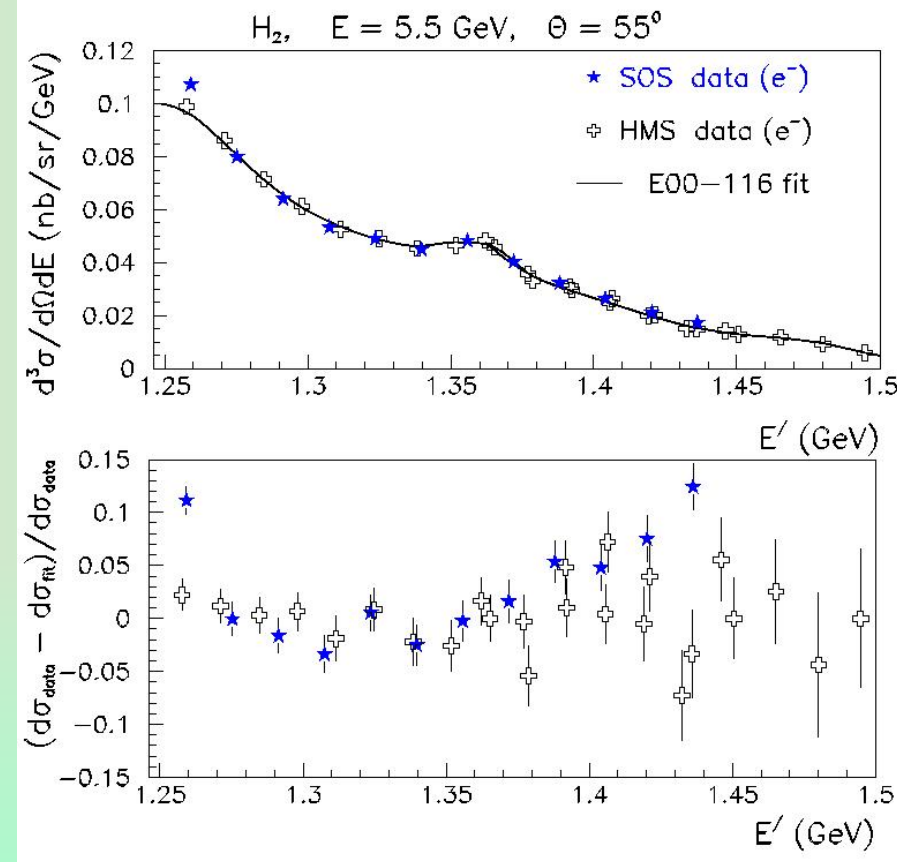
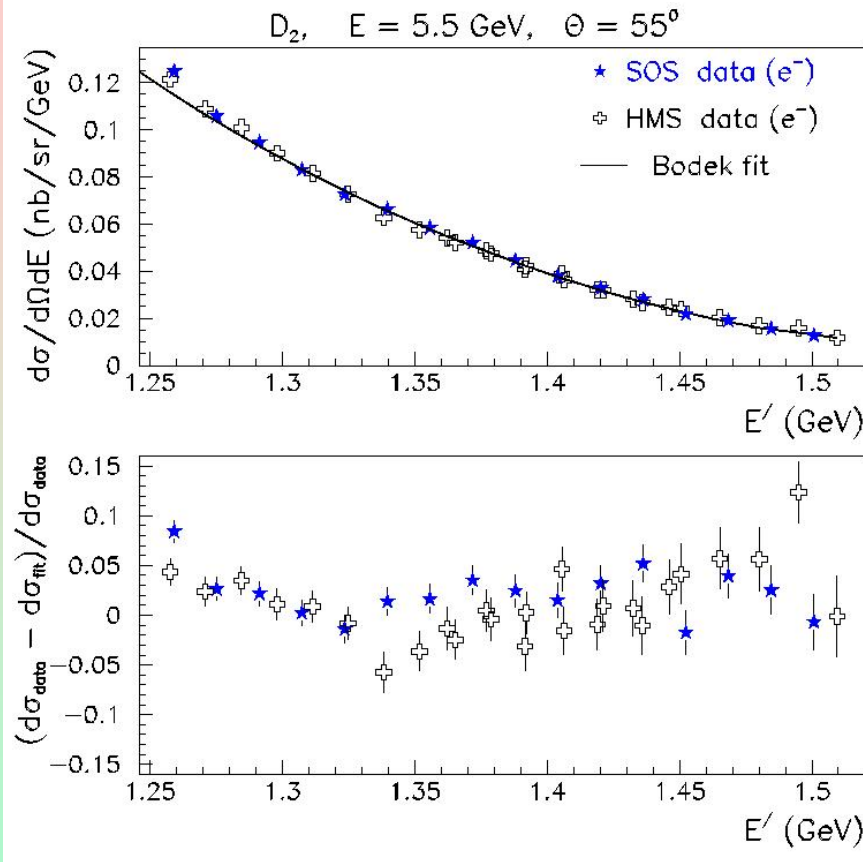
**based on Wiser  $\pi^+, \pi^-$  production data)**

The positron cross section is subtracted from the measured electron cross section on a  $(\delta, \theta)$  grid.





# Charge Symmetric Background: Quality Checks



Quality check: compare the same physics taken in different spectrometers.  
HMS analysis agrees with SOS analysis in within 1.3% for both targets.

Systematic uncertainty on the positron cross section: 6% (38,41,45,55)  
and 20% (60,70)  $\Rightarrow$   $<0.2\%$  (38,41,45,55) and  $<2.5\%$  for (60,70) on the  
electron cross section.



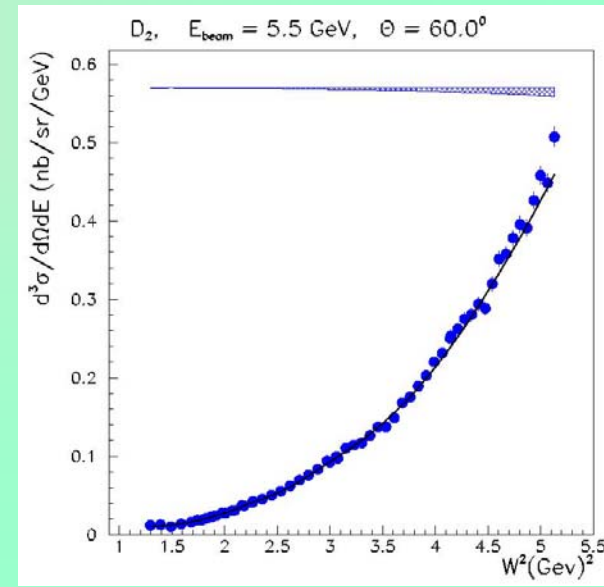
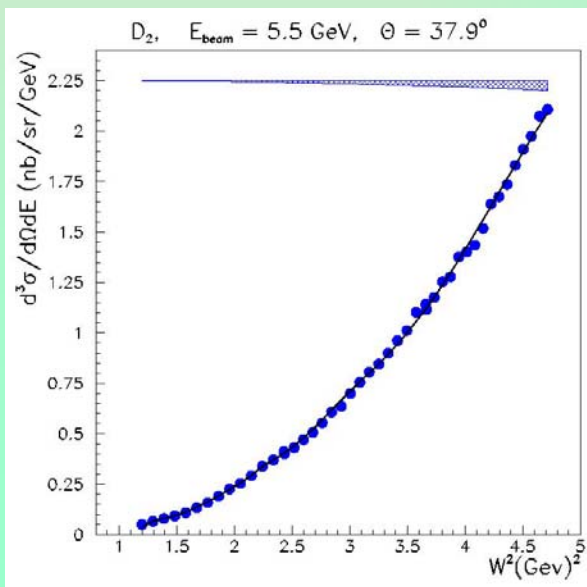
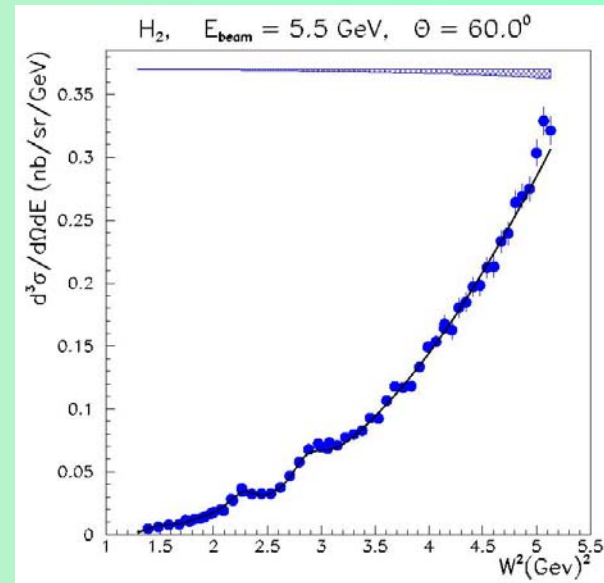
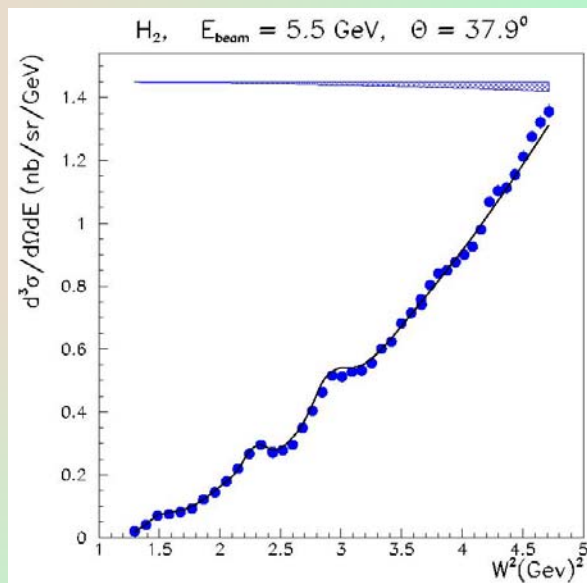
# Differential Born inelastic cross sections extracted from E00-116 measurements

Proton fit shown: M.E.  
Christy fit after last  
iteration

Deuteron fit shown:  
E00-116 fit after the  
last iteration.

The systematic point-  
to-point uncertainty is  
shown as a band: up to  
5% at large  $x$ .

The normalization  
uncertainty: 1.75%.





## F<sub>2</sub> Extraction

$$F_2 = \frac{d^3\sigma}{d\Omega dE'} \frac{1+R}{1+R\varepsilon} \frac{K\nu}{4\pi^2\alpha} \frac{1}{\Gamma} \frac{1}{1+\nu^2/Q^2}$$

E00-116 measures

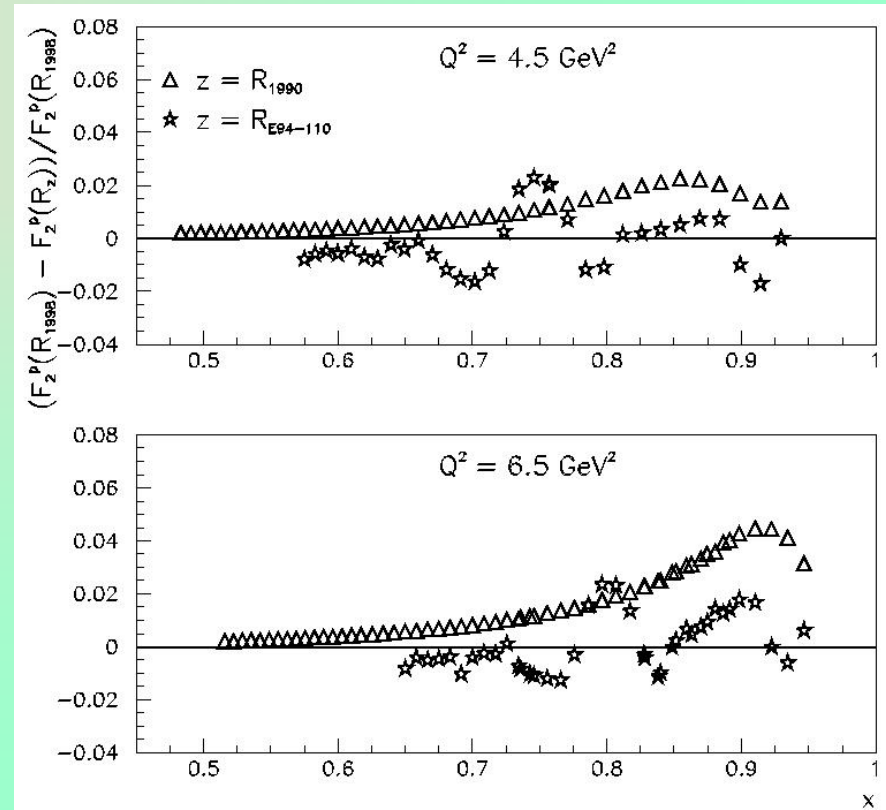
We wish to construct F<sub>2</sub> but have not measured R.

kinematic term

For F<sub>2</sub> extraction R1998 was used.

To estimate uncertainty: calculated F<sub>2</sub> with 3 different R parameterizations

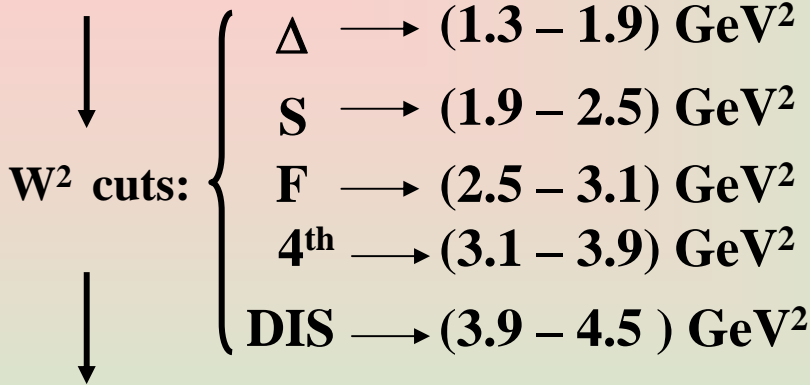
Estimated uncertainty on F<sub>2</sub> originating from the R parameterization used is about 2%.





# F<sub>2</sub> Results and Averaging

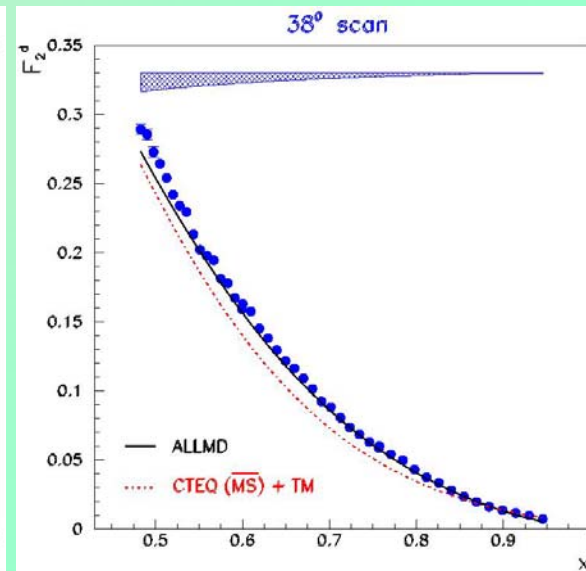
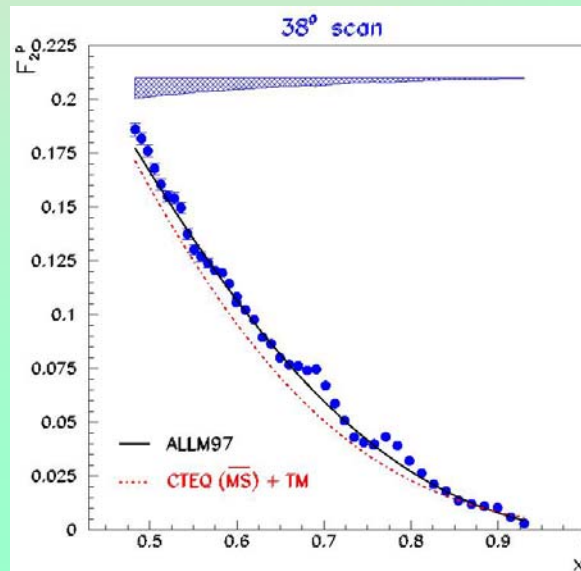
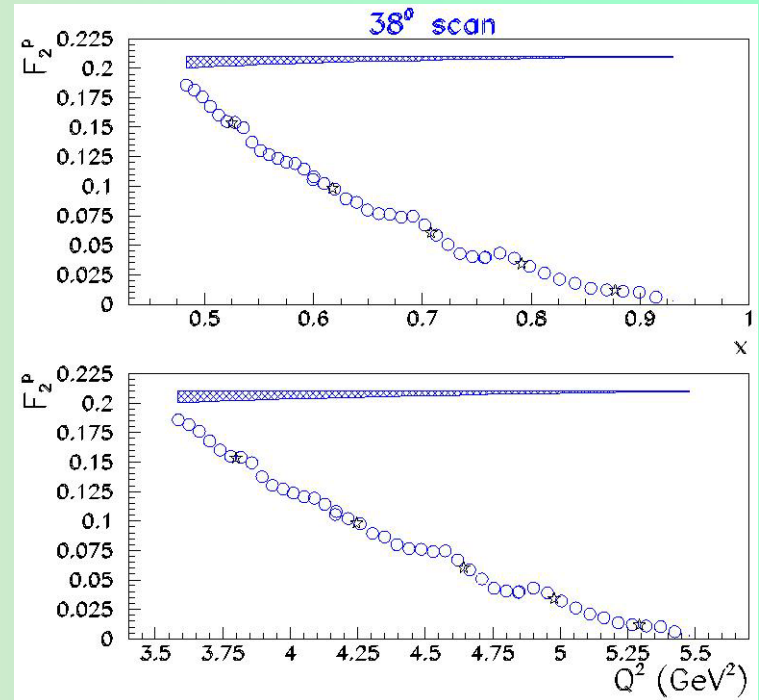
These



were used to average over each dis / resonance "region", for a given scan, in order to obtain F<sub>2</sub><sup>average</sup>.

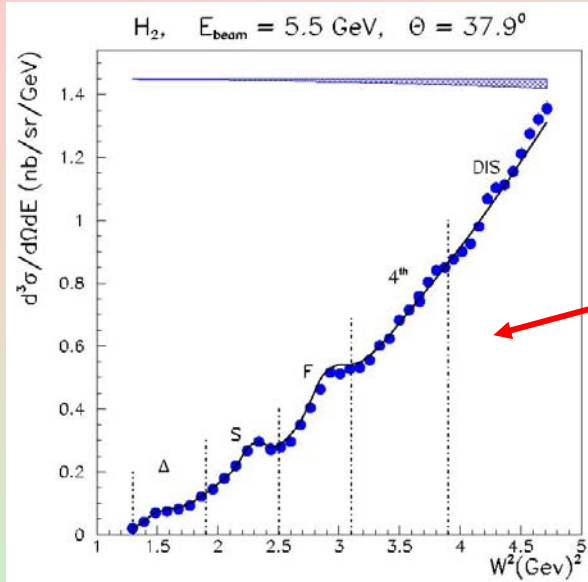
$$F_2^{average} = \frac{\int_{x_{min}}^{x_{max}} F_2 dx}{\int_{x_{min}}^{x_{max}} dx}$$

$$x_{average} = \frac{\int_{x_{min}}^{x_{max}} x dx}{\int_{x_{min}}^{x_{max}} dx}$$



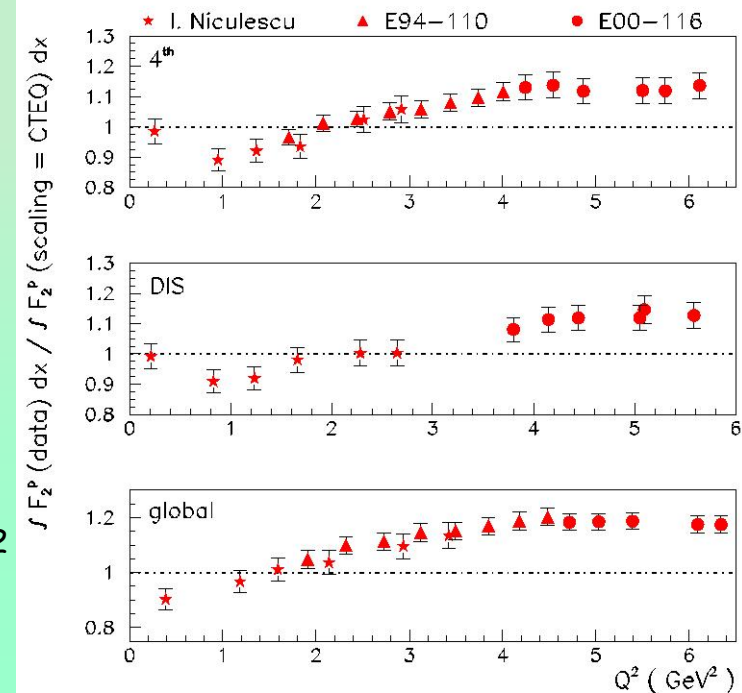
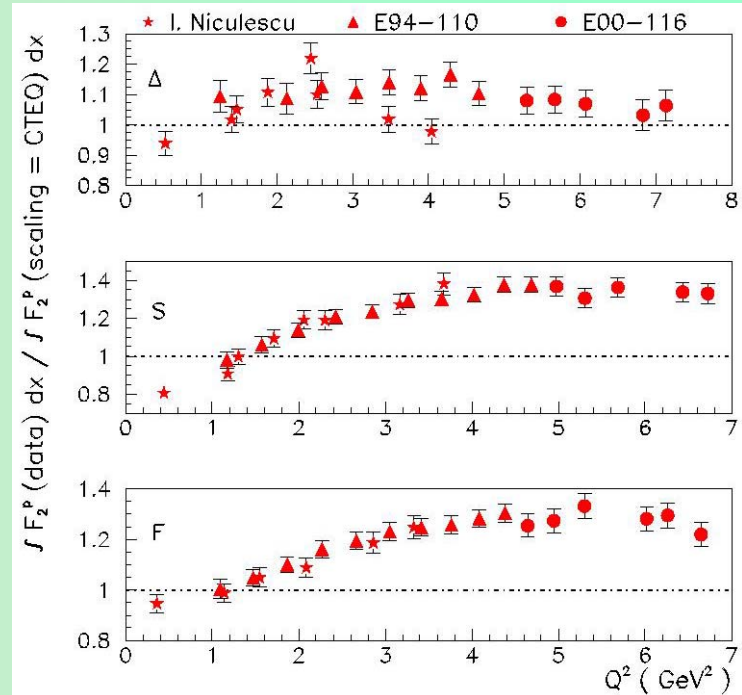


# Quark-Hadron Duality Studies (CTEQ6 + TM)



$$I = \frac{\int_{x_{\min}}^{x_{\max}} F_2^{\text{data}} dx}{\int_{x_{\min}}^{x_{\max}} F_2^{\text{paramet.}} dx}$$

paramet. = CTEQ6 +  
TMC & ALLM97



## Globally:

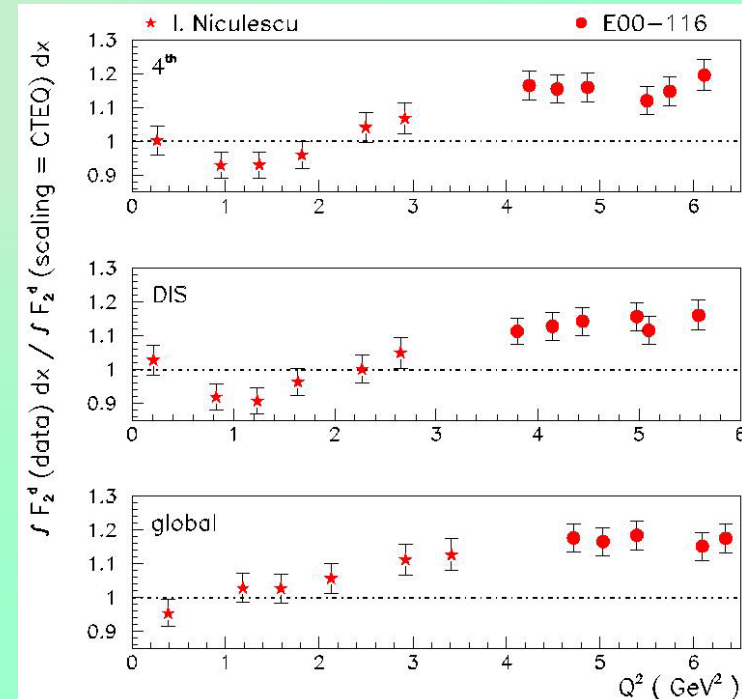
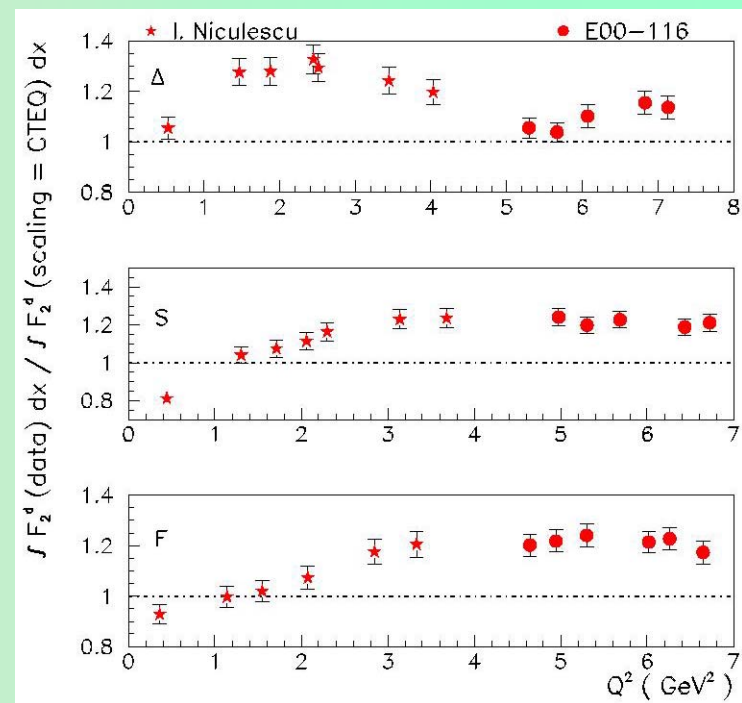
- $I$  falls below unity for  $Q^2 < 1 \text{ GeV}^2$  :
- $Q^2 \sim 1.5 \text{ GeV}^2$ ,  $I \sim 1$
- $I$  reaches a plateau at  $Q^2 \sim 4 \text{ GeV}^2 \Rightarrow$   
CTEQ6 not constrained quantitatively at large  $x$   
and intermediate  $Q^2$  but seems to describe  
qualitatively the  $Q^2$  dependence above  $Q^2 > 4 \text{ GeV}^2$



# Quark-Hadron Duality Studies (CTEQ6 + TM)

## Locally:

- $I$  saturates at constant value for  $Q^2 > 4$   $\text{GeV}^2$  but different for each resonance region!  $\Rightarrow$
- ❖ the  $Q^2$  dependence -described qualitatively to some degree for each resonance region for  $Q^2 > 4$   $\text{GeV}^2$ .
- ❖ locally might be residual  $Q^2$  effects which cannot be described by pQCD fit.
- N- $\Delta$  transition awkward behavior compared to the rest of the resonance regions (previously reported).





# Quark-Hadron Duality Studies (ALLM97)

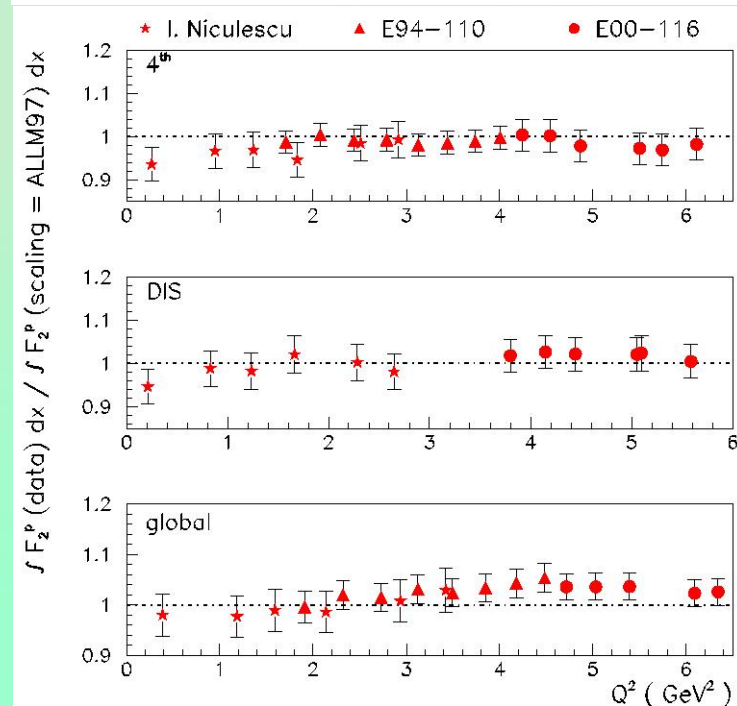
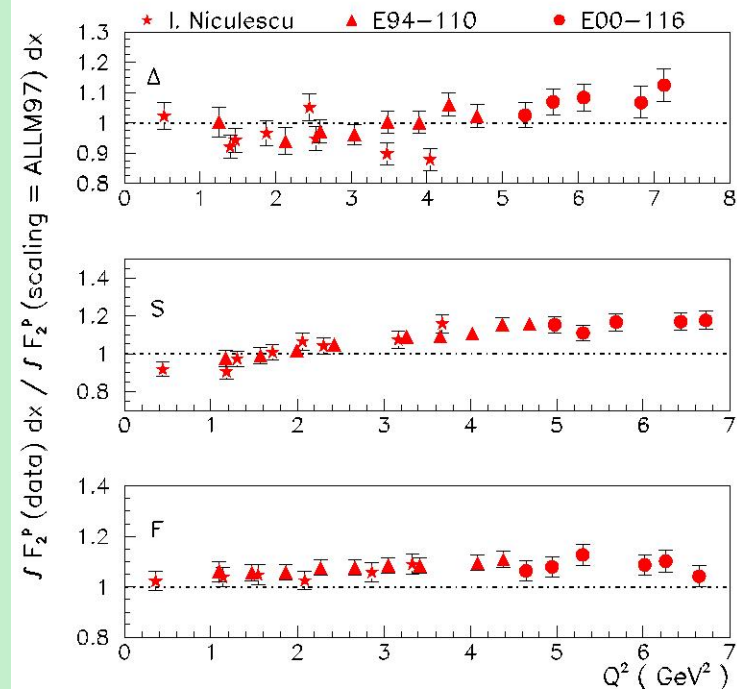
## Globally:

➤ I around 1 within 2-2.5% (both proton and deuteron) for the entire  $Q^2$  range down to the lowest  $Q^2 \sim 0.4 \text{ GeV}^2$ .

➤ ALLM97 can include nonperturbative effects (fit to low  $W^2$  DIS data)  $\Rightarrow$  explains the "observation of duality" down to such a low  $Q^2$ .



❖ globally, on average, the nonperturbative effects in the RES region seem to be quantitatively comparable with the ones in DIS.





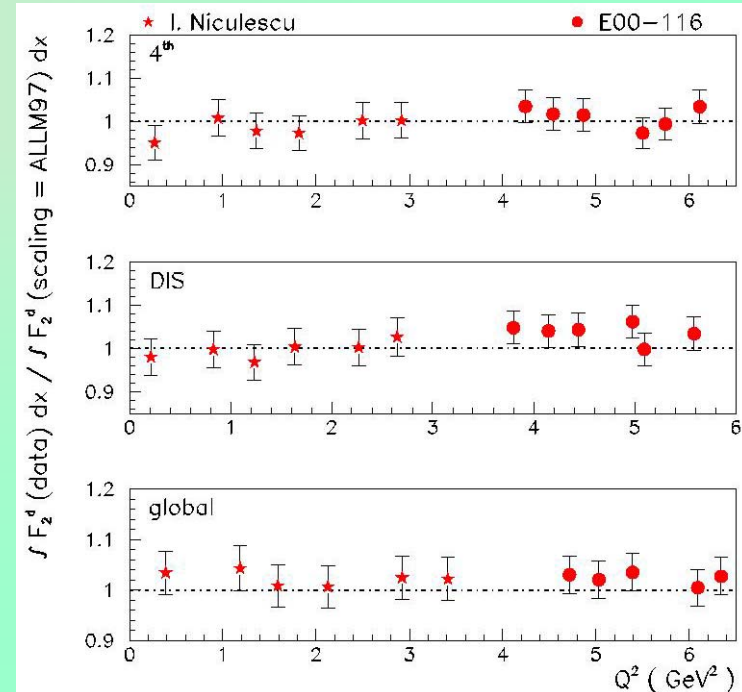
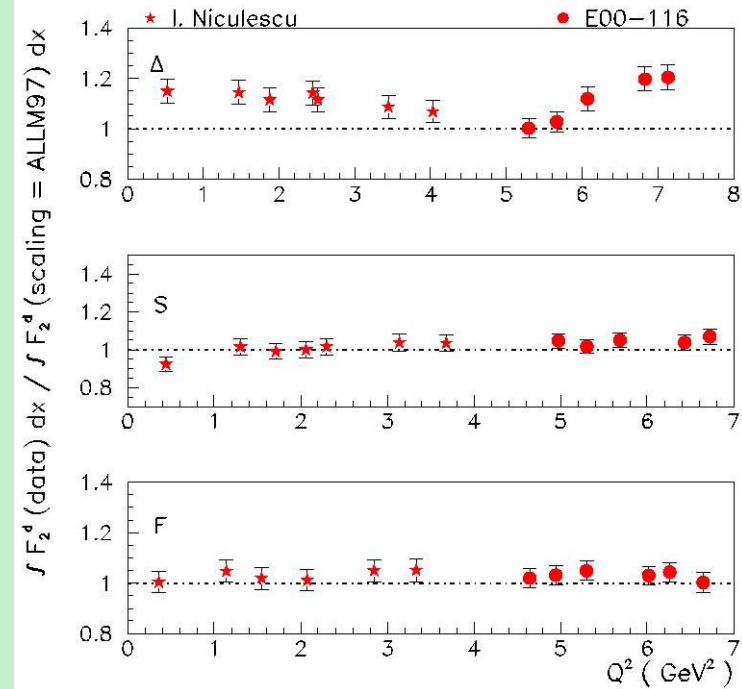
# Quark-Hadron Duality Studies (ALLM97)

## Locally:

- I close to unity within 2% for both DIS and forth resonance region for most of the  $Q^2$  range analyzed.
- For the rest of the RES regions, I rises above unity with increasing  $Q^2$  more prominently.



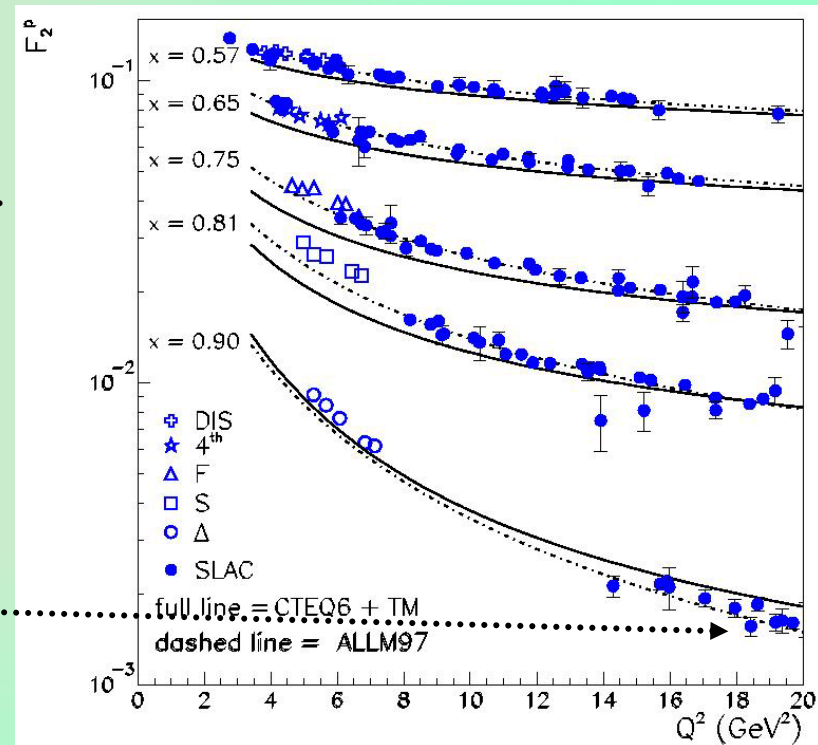
- ❖ larger  $Q^2$  corresponds to larger  $x$  where ALLM97 not constrained.
- ❖ ALLM97 goes to 0 at  $x=1$   $\Rightarrow$  type of fit function bound to fail at large  $x$  in describing data (does not account for the kinematic HT).





## $Q^2$ -evolution of $F_2$

- Quantitative discrepancy (up to 40%) between data and pQCD fit at large  $x$  and intermediate  $Q^2$  (LxR not taken into account).
- Qualitatively, the  $Q^2$  dependence described to some degree, at least for each resonance region separately.
- pQCD fit fails to describe data at large  $x$  and higher  $Q^2$ .



ALLM97 -better quantitative agreement with the data, as expected.



# Twist-4 Extraction (work in collaboration with S. Liuti)

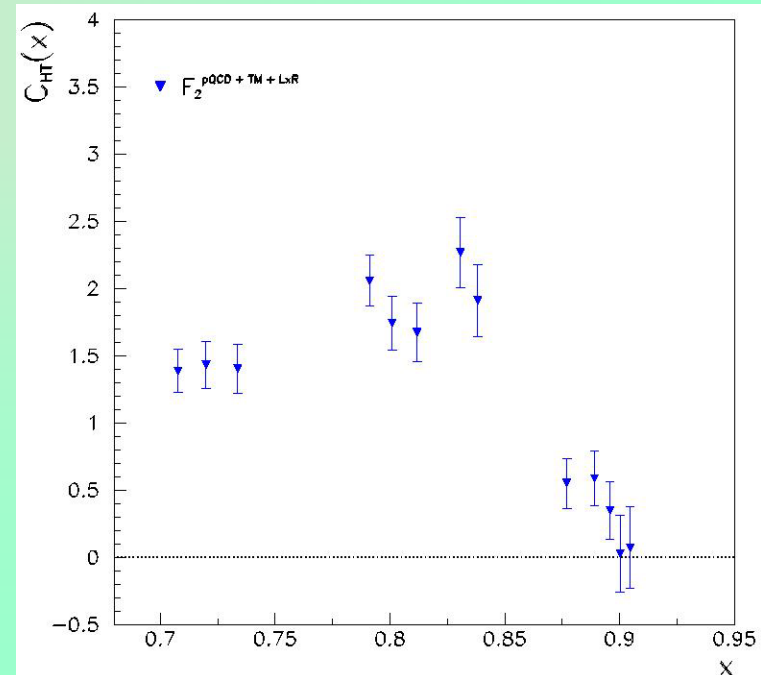
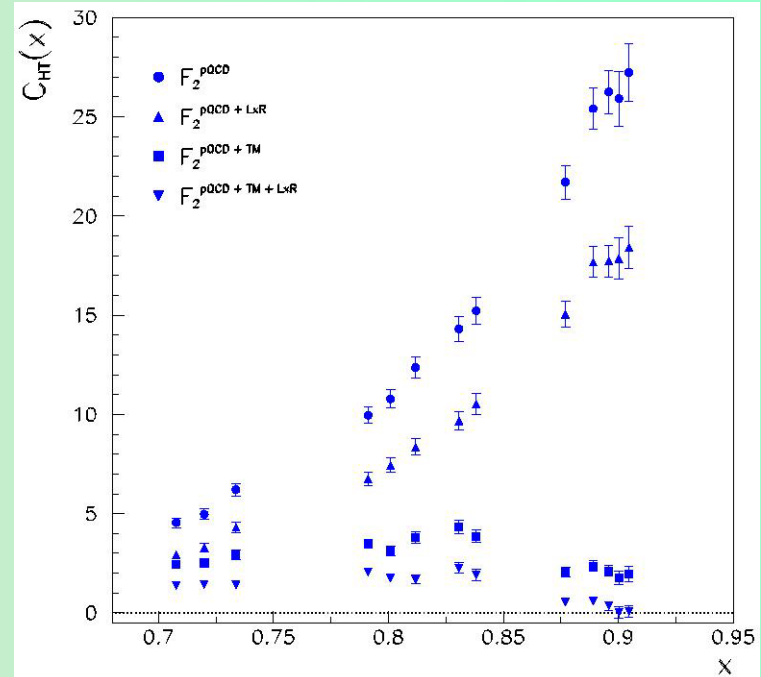
pQCD  
leading twist  
+ TM + LxR

$$F_2^{pQCD+TM} = 1 + \frac{C_{HT}(x)}{Q^2}$$

➤ The regions with decreasing invariant mass are characterized by lower values of twist-4 coefficient (particularly evident for  $\Delta$ ).

➤ Discrepancies between the DIS and RES twist-4 was reported before, where the global duality including integrations over the whole low- $W^2$  was studied.

➤ The accuracy of the present data (smaller bins in  $W^2$ ) quantitatively points for the first time at the  $\Delta$  contribution as possible origin of the discrepancy.





## Conclusions

“Technical” analysis of the data: completed.  $\rightarrow F_2$  structure functions (proton and deuteron) in the resonance region with  $x \rightarrow (0.54 - 0.94)$  and  $Q^2 \rightarrow (3.8 - 7.2) \text{ GeV}^2$ .

### Physics studies revealed:

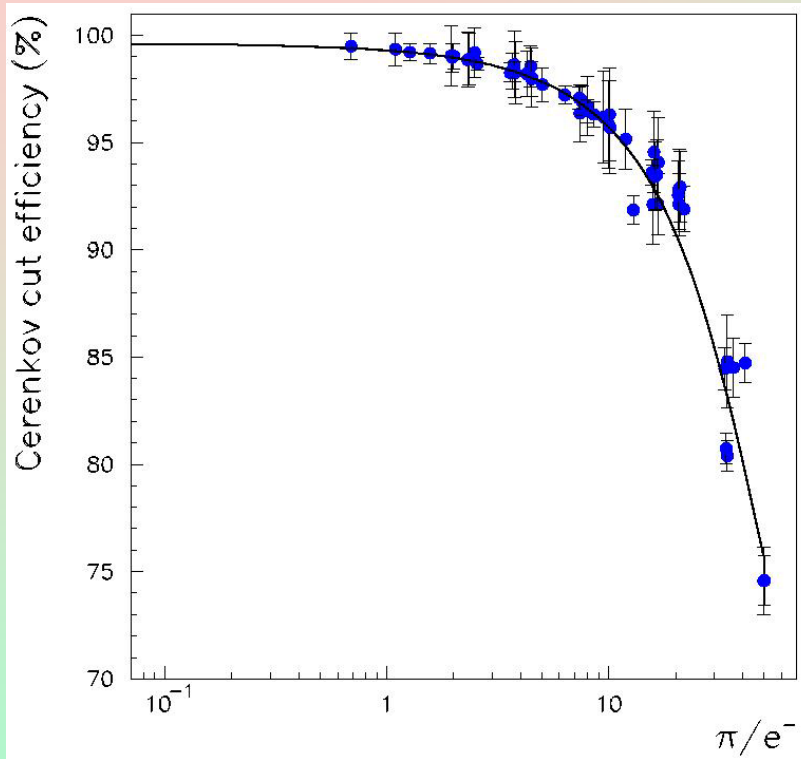
- HT effects in resonance region are, on average, comparable to the ones in DIS (global duality studies).
- - pQCD fits and empirical parameterizations not constrained at large  $x$  and intermediate  $Q^2$  (local duality studies).

**The twist-4 was extracted from the first, second and third resonance region data:**

- the regions with decreasing invariant mass are characterized by lower values of twist-4 coefficient (particularly evident for  $\Delta$ ).
- discrepancies between the DIS and RES twist-4 was reported before  $\rightarrow$  the accuracy of the present data (smaller bins in  $W^2$ ) quantitatively points for the first time at the  $\Delta$  contribution as possible origin of the discrepancy.



## Cerenkov efficiency



PID cut for electron selection:  $hcer\_npe > 2$   
Do we reject any electrons with this cut?  
We need a clean sample of electrons to estimate the cut efficiency.

Problem for E00-116 (low momentum so we have high  $p/e$  ratio): we cannot select a clean sample of electrons using just the shower counter.

$$\varepsilon_{Cerenkov} = \frac{N(hcer\_npe > 2 \ \& \ hsshtrk > 0.9)}{N(hsshtrk > 0.9)}$$

$$\frac{\pi}{e} = \frac{N(hcer\_npe = 0)}{N(hcer\_npe > 12)}$$

We extrapolate the "efficiency" at zero  $\pi/e$  ratio  $\Rightarrow$  real efficiency

**E00-116:  $\varepsilon = (99.63 \pm 0.24) \%$**



## Calorimeter efficiency

PID cut for electron selection:  $hsshtrk > 0.7$

Do we reject any electrons with this cut?

We need a clean sample of electrons to

estimate the cut efficiency.

Problem for E00-116: we cannot select a clean sample of electrons using just the Cerenkov detector.

$$\mathcal{E}_{total} = \mathcal{E}_1 \cdot \mathcal{E}_2$$

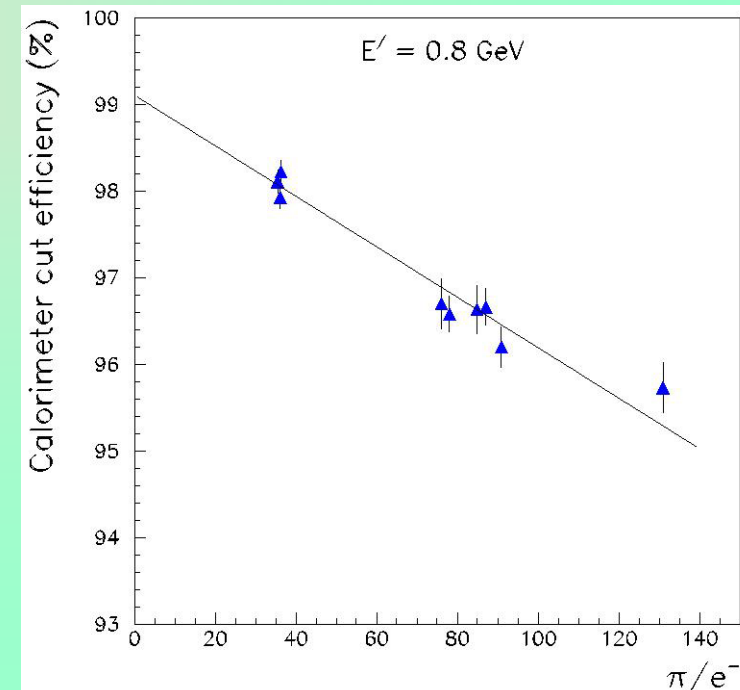
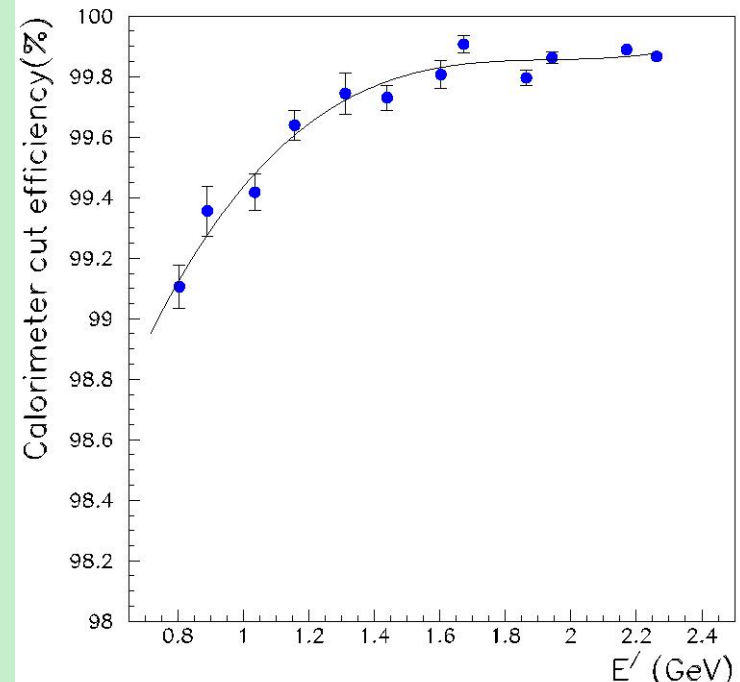
$$\mathcal{E}_1 = \frac{N(hsshtrk > 0.7 \ \& \ hcer\_npe > 12)}{N(hcalet > 0.7 \ \& \ hcer\_npe > 12)}$$

$$\mathcal{E}_2 = \frac{N(hcalet > 0.7 \ \& \ hcer\_npe > 12)}{N(hcalet > 0.5(0.25) \ \& \ hcer\_npe > 12)}$$

For each fixed momentum (separate the pion cont. dependence of the eff. from the resolution dependence) we get  $e_{tot}$  at  $\pi/e = 0$ .

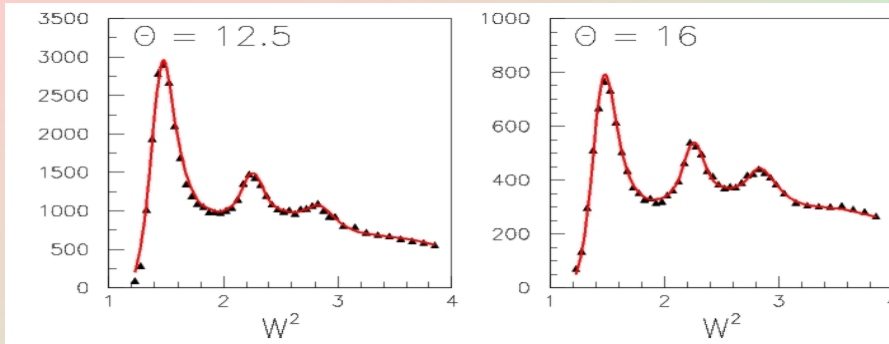
**Point-to-point systematic = 0.25%**

**Normalization systematic = 0.3%**





# Iteration procedure

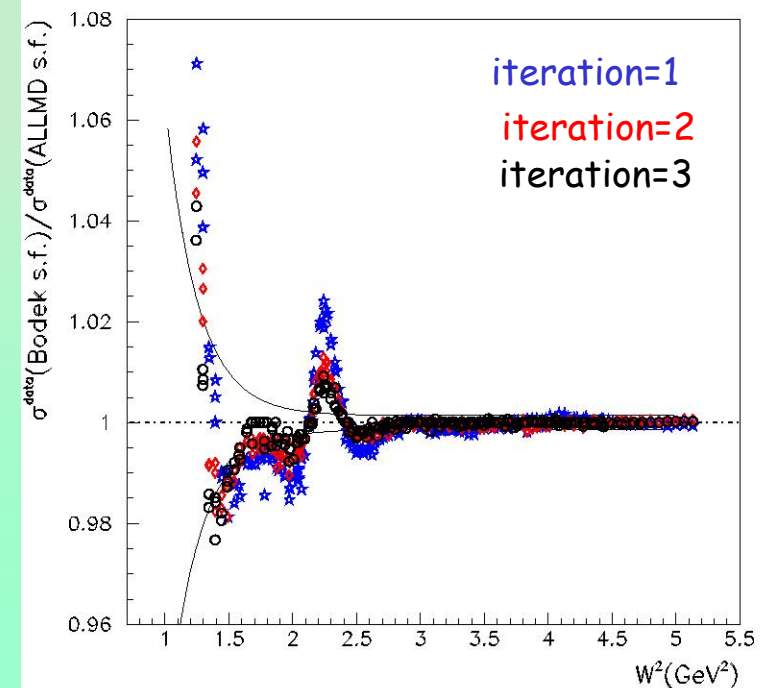
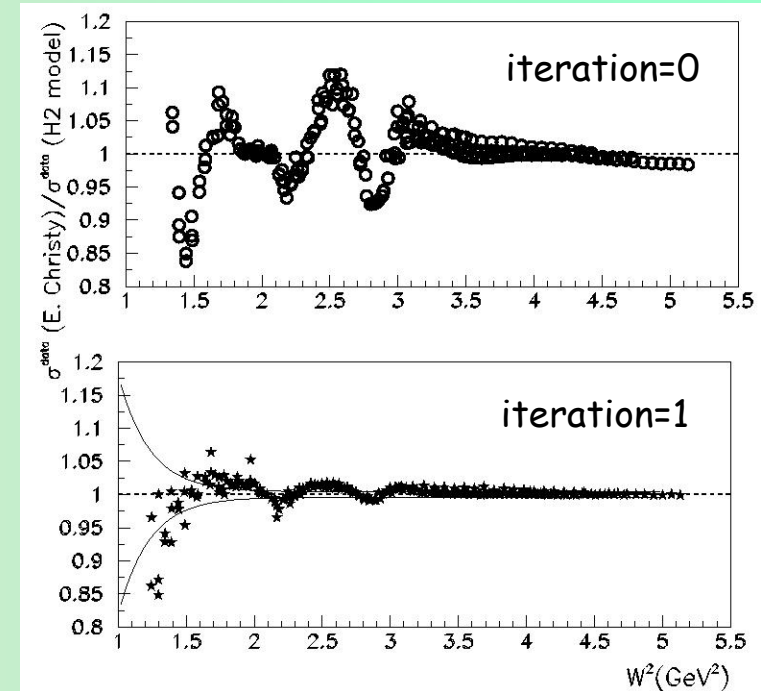


1 iterations for proton data (M.E. Christy fit procedure used): with two starting models -M.E. Christy model and h2\_model.

3 iterations for deuteron data (M.E. Christy fit procedure used): with two starting models -Bodek and ALLM\*d/p model.

Systematic uncertainty:

- proton: 0.2% at high  $W^2$  but increasing up to 2.5% for  $W^2=1.5 \text{ GeV}^2$ .
- deuteron: 0.2% at high  $W^2$  but increasing up to 2% for  $W^2=1.3 \text{ GeV}^2$ .





# Tracking efficiency checks

Tracking inefficiency: tracking algorithm fails to reconstruct a track when a trigger occurs

$$\mathcal{E}_{tracking} = \frac{N_{DID}}{N_{SHOULD}}$$

electrons selected with PID cuts

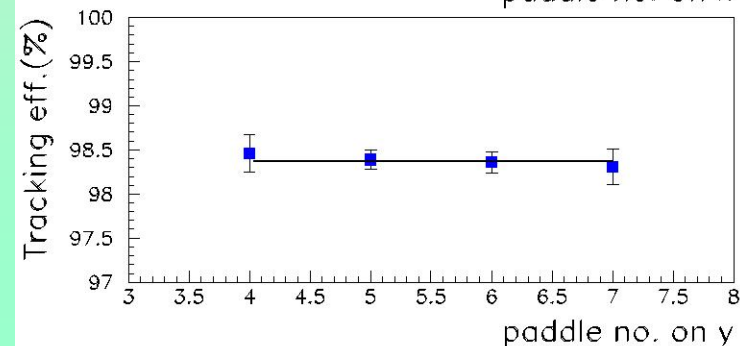
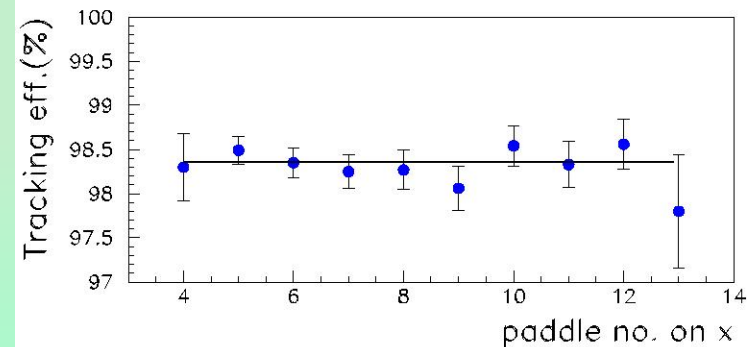
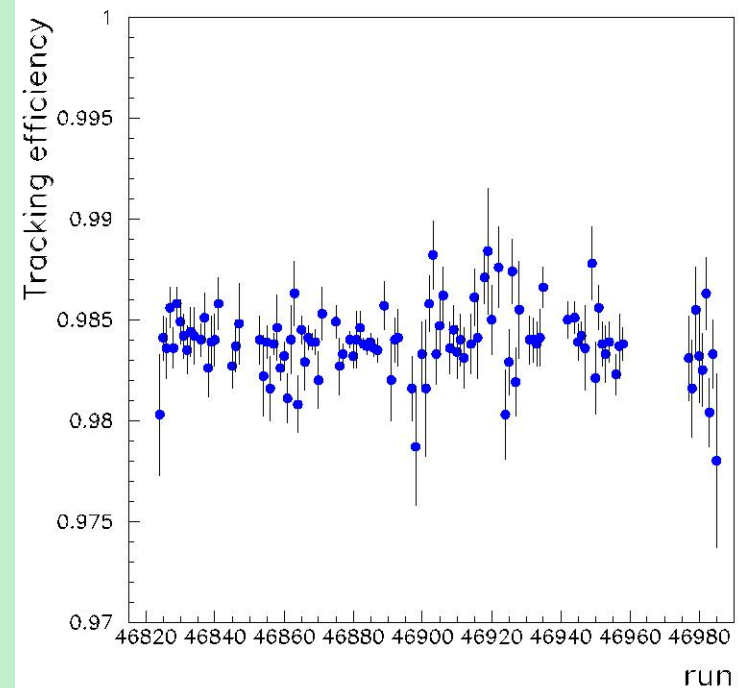
We are at low rates so we don't worry about the rate dependence of the tracking efficiency.

But the tracking efficiency **could** have an angle dependence (small angle approximation used in the tracking algorithm).

We don't see any angle dependence in the tracking efficiency.

We use a linear fit instead of run-by-run efficiency because of the large statistical fluctuations.

$$\mathcal{E}_{tracking} = (98.4 \pm 0.2)\%$$



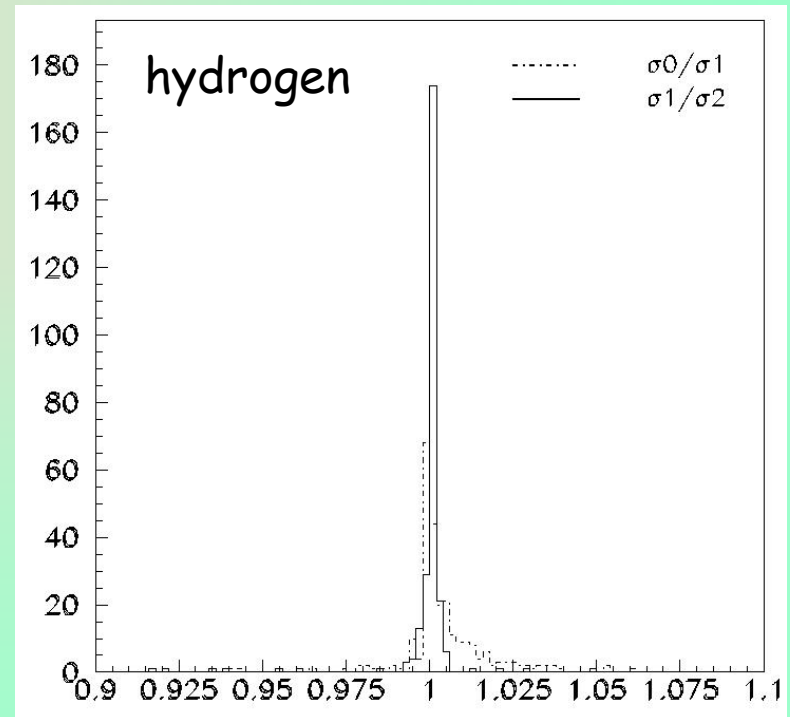
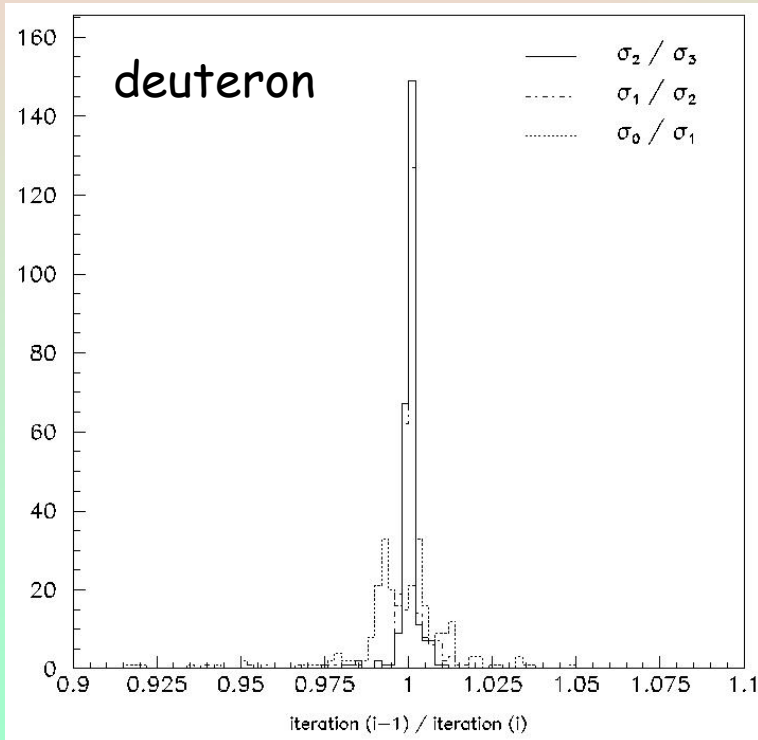


## Iteration Procedure

Model used for  
Bin-centering correction =>  
and radiative corrections  
Calculation.

$$\sigma_{BC}^i(E, E', \theta_c) = \sigma^{data}(E, E', \theta_i) \frac{\sigma_{model}(E, E', \theta_c)}{\sigma_{model}(E, E', \theta_i)}$$

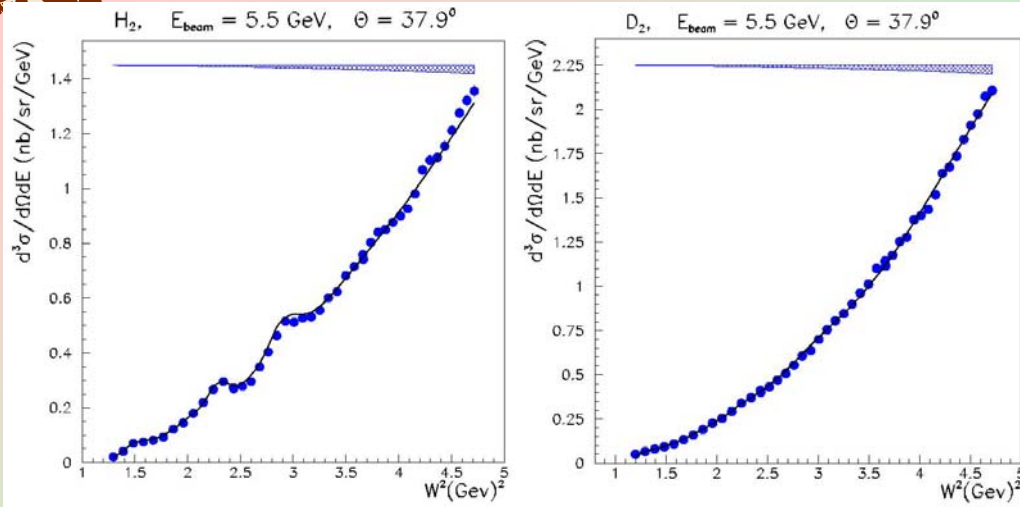
statistically averaged to obtain:  $\sigma(E, E', \theta_c)$



Necessary to minimize the model dependence of the extracted cross section (cross section models are used for bin-centering and radiative correction calculation).



# Iteration procedure

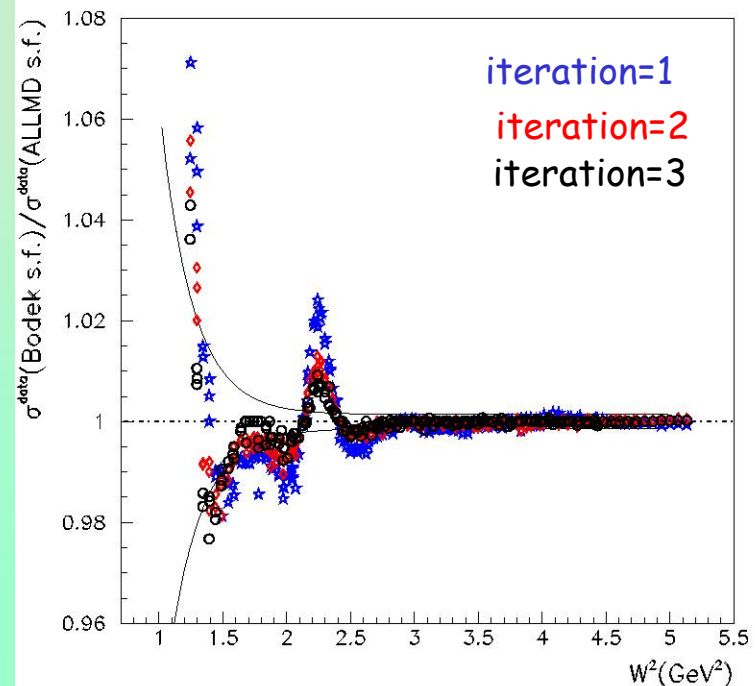
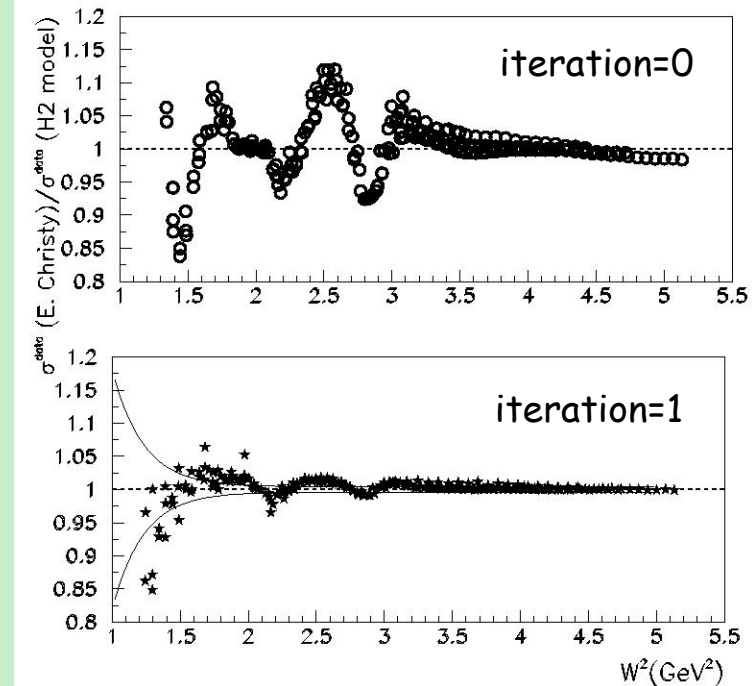


1 iterations for proton data (M.E. Christy fit procedure used): with two starting models -M.E. Christy model and h2\_model.

3 iterations for deuteron data (M.E. Christy fit procedure used): with two starting models -Bodek and ALLM\*d/p model.

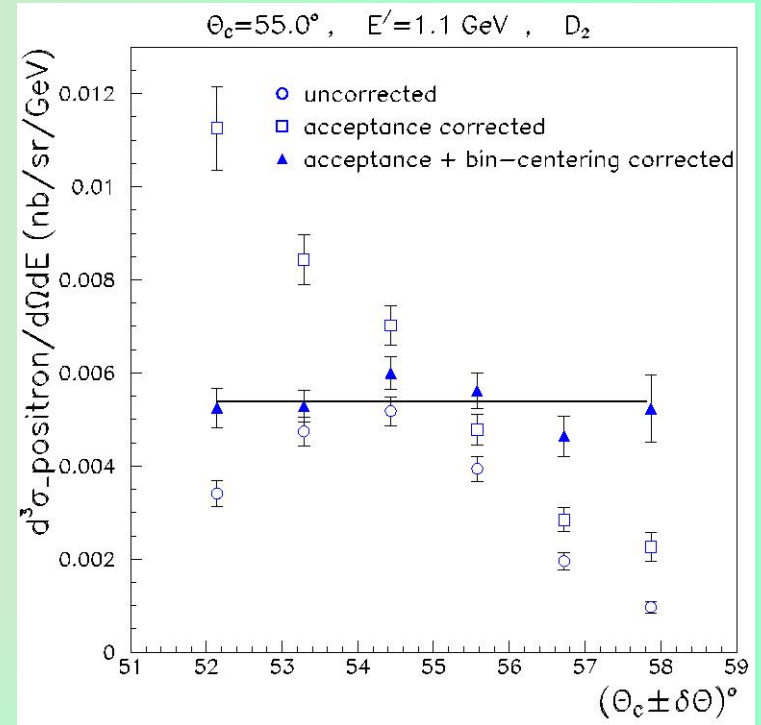
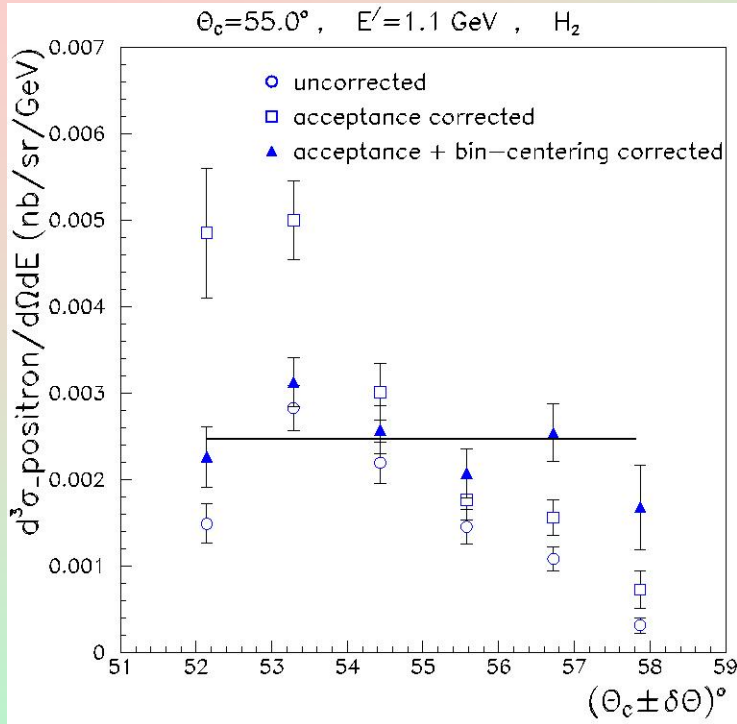
Systematic uncertainty:

- proton: 0.2% at high  $W^2$  but increasing up to 2.5% for  $W^2=1.5 \text{ GeV}^2$ .
- deuteron: 0.2% at high  $W^2$  but increasing up to 2% for  $W^2=1.3 \text{ GeV}^2$ .





# Charge symmetric background: quality checks



Bin-centering correction: 
$$\sigma_{BC}^i(E, E', \theta_c) = \sigma^{data}(E, E', \theta_i) \frac{\sigma_{model}(E, E', \theta_c)}{\sigma_{model}(E, E', \theta_i)}$$

statistically averaged to obtain:  $\sigma(E, E', \theta_c)$

P. Bosted model describes reasonably well the positron cross section in the angular acceptance at this experiment kinematics.



# Pion Contamination Calculation

PID cuts used for electron selection



$hsshtrk > 0.7$   
 $hcer\_npe > 2$

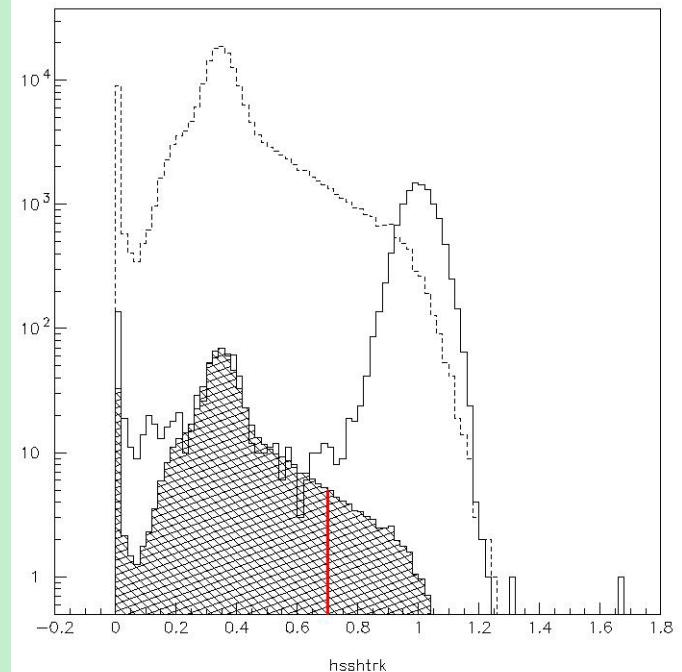
We are at large angles so the  $(e, e^-)$  cross section is typically low.

We are at low momentum so we have high  $\pi/e$  ratio.

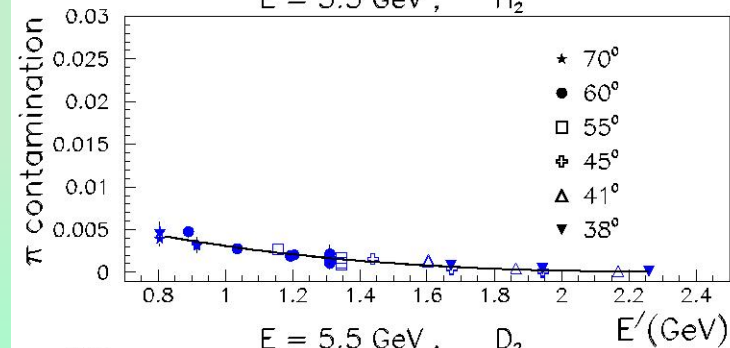
The typical PID cuts don't clean up all the pions.

We assume that for  $hcer\_npe < 2$  we have only pions and for  $hcer\_npe > 2$  still some pion contamination  $\rightarrow$  we "scale" the pion spectrum to subtract pions.

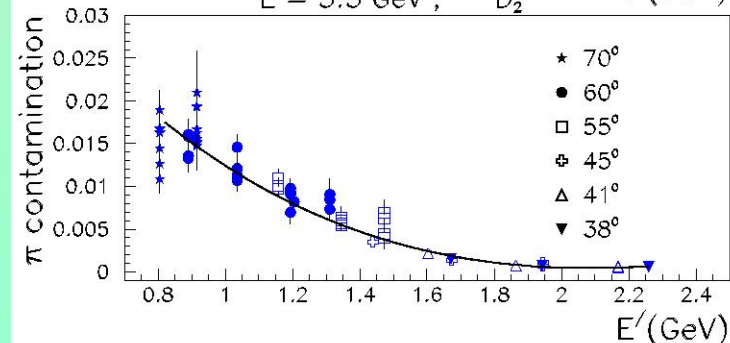
The pion contamination is parameterized as a function of momentum and the fit is used for correction.



$E = 5.5 \text{ GeV}, H_2$



$E = 5.5 \text{ GeV}, D_2$





# Moments of the Structure Function

Moments of the  $F_2$  Structure Function:

$$M_2^{(n)}(Q^2) = \int_0^1 dx x^{n-2} F_2(x, Q^2)$$

➤ elastic contribution dominates the moments at low  $Q^2$  but falls off rapidly at larger  $Q^2$ .

➤ without elastic contribution (highly nonperturbative effect) the  $Q^2$  dependence of the moments is rather shallow down to low  $Q^2 \Rightarrow$

❖ the nonperturbative corrections to the  $Q^2$  dependence small on average.

